

# Joule heating induced negative differential resistance in free standing metallic carbon nanotubes

Marcelo A. Kuroda

*Beckman Institute and Department of Physics, University of Illinois Urbana-Champaign, IL 61801*

Jean-Pierre Leburton\*

*Beckman Institute and Department of Electrical and Computer Engineering,  
University of Illinois Urbana-Champaign, IL 61801*

(Dated: July 15, 2018)

The features of the  $IV$  characteristics of metallic carbon nanotubes (m-NTs) in different experimental setups are studied using semi-classical Boltzmann transport equation together with the heat dissipation equation to account for significant thermal effects at high electric bias. Our model predicts that the shape of the m-NT characteristics is basically controlled by heat removal mechanisms. In particular we show that the onset of negative differential resistance in free standing nanotubes finds its origins in strong transport nonlinearities associated with poor heat removal unlike in substrate-supported nanotubes.

Since their discovery [1], carbon nanotubes (NTs) have captured the attention of both the scientific and technological communities because of their mechanical stability as well as their high thermal and electrical capabilities [2] not usually seen in other materials. Among their outstanding properties is the peculiarity to behave as metals or semiconductors depending on their chirality [3, 4]. Their capability of carrying large current densities at room temperature make them prominent materials for field effect transistors [5, 6] and interconnects [7] in high speed nanoscale electronics. The first measurements of the  $IV$  characteristics on individual metallic nanotubes (m-NTs) [8] were performed on substrate-supported tubes in a configuration similar to a field effect transistor. The output characteristics resembled those obtained in semiconductors as they exhibited linear dependence on voltage in the low field regime, and saturation at  $I \sim 25 \mu\text{A}$  under high biases. Later measurements have shown that in short m-NTs, the saturation level could be overcome, but a nonlinear behavior still persists in substrate-supported configurations [9, 10]. In recent experiments performed on m-NTs standing freely across a trench, current levels in the high bias regime were a few times smaller than those in nanotubes supported by substrates while negative differential resistance (NDR) was reported [11]. This behavior, indicating significant heat production/dissipation in m-NTs devices, was interpreted in terms of the onset of a non-equilibrium optical phonon population.

In this Letter we show that the nonlinearities in the  $IV$  characteristics of m-NTs, find their origins in Joule heating and the efficiency in heat removal from the m-NT. We determine the temperature profile along nanotubes by solving the Boltzmann transport equation simultaneously with the heat transfer equation. We specifically demonstrate that while the nonlinear behavior in substrate-supported tubes (SSTs) (Fig. 1.a) emerges due to a strong imbalance between carrier distribution func-

tions with positive and negative Fermi velocity, the characteristics in free-standing tubes (FSTs) (Fig. 1.b) essentially arise from an inhomogeneous self-heating effect.

The distance between sub-bands in m-NTs using tight-binding calculations can be estimated as  $\Delta E_{met} \approx 6\gamma_0 a/D$  where  $a = 0.14 \text{ nm}$ ,  $\gamma_0 \approx 3 \text{ eV}$  and  $D$  is the diameter of the tube [12]. Hence, for transport purposes, the electronic structure of small diameter m-NTs close to the Fermi level can be well described by linear dispersion relations  $E(k) = \pm \hbar v_F (k - k_F)$  with a Fermi velocity  $v_F$  close to  $8 \cdot 10^7 \text{ cm/s}$ . This approximation is valid as long as temperature satisfies that  $k_B T \ll \Delta E_{met}$  and the bias voltage  $V < \Delta E_{met}$ . The current along the nanotube is naturally defined as:

$$I = e v_F (n^+ - n^-) \quad (1)$$

where  $n^+$  ( $n^-$ ) is the electron density with positive (negative) Fermi velocity. Similarly to Ref. [13], we assume that carrier populations are described by Fermi statistics with different quasi-Fermi level  $E_F^\alpha$  depending on the sign  $\alpha$  of the Fermi velocity. Using the zeroth moment of the Boltzmann equation, the electric field  $F$  satisfies:

$$v_F \partial_x (n^+ + n^-) - \frac{2eF}{\pi \hbar} = 2\tilde{C}_{ph}(I, T). \quad (2)$$

Here  $\tilde{C}_{ph}(I, T)$  is the momentum integral of the collision integral considering only the contribution to scattering involving high energy optical phonons ( $\hbar\omega \sim 0.18 \text{ eV}$ ). In our model, phonons are assumed to be in *local* thermal equilibrium with electrons, and their occupation number follows the Bose-Einstein statistics.

A realistic description of the  $IV$  characteristics requires the consideration of the temperature profile  $T(x)$  along the m-NT in the right hand side of Eq. 2. We account for this local temperature variation by solving the heat production/dissipation equation:

$$-\frac{d}{dx} \left( \kappa \frac{dT}{dx} \right) + \gamma (T - T_0) = q^*, \quad (3)$$

in which  $\kappa$ ,  $\gamma$ ,  $T_0$ , and  $q^*$  are the thermal conductivity, the thermal coupling to the substrate, the substrate temperature, and the heat dissipation per unit volume, respectively. The first term on the left hand side of Eq. 3 corresponds to the heat flowing through the leads; the second, to the flow driven through the substrate or any surrounding medium. The heat produced locally is assumed to obey Joule's law  $q^* = IF/\pi Dt$ , being  $t$  the effective thickness of the tube ( $t \approx 0.34\text{nm}$ ). The m-NT thermal conductivity dependence on temperature has been predicted to follow  $\kappa(T) = \kappa_{RT}T_{RT}/T$ , due to the Umklapp process of acoustic phonons [14] for  $T \gtrsim 300\text{K}$ . In this equation,  $\kappa_{RT}$  is the thermal conductivity at a reference temperature  $T_{RT}$  ( $\kappa \sim 20\text{W/cmK}$  at  $300\text{K}$ ). An estimate of the thermal coupling constant  $\gamma$  of nanotubes standing on  $\text{SiO}_2$  substrates is  $10^{11}\text{W/cm}^3\text{K}$  [13]. The explicit dependence of the temperature on the local field requires Eqs. 2 and 3 to be solved simultaneously, leading to a non-linear second order differential equation for the temperature. We set the boundary conditions as  $T(\pm L/2) = T_0$ , where  $L$  is the m-NT length, assuming that both contact leads have the same temperature as the substrate (i.e. we neglect the heating at the leads due to a contact resistance).

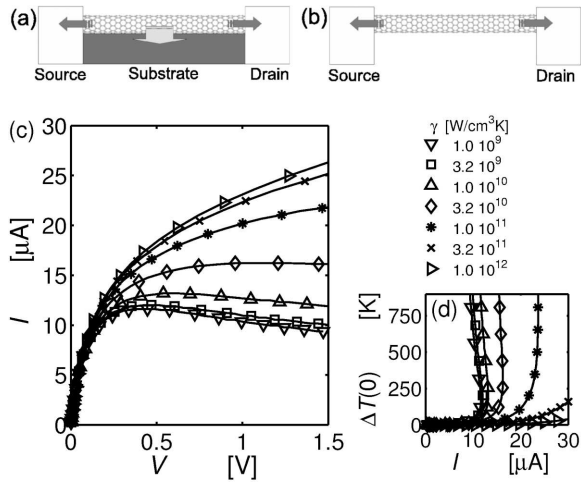


FIG. 1: Experimental setups: (a) Substrate-supported nanotube (SST); (b) Free-standing nanotube (FST). (c)  $IV$  characteristics for 800nm-long nanotube with different values of coupling coefficient  $\gamma$ . (d) Temperature in the middle of the tube  $\Delta T(0)$  as a function of the current  $I$  for different  $\gamma$ .

In Fig. 1(c) we compare the performances of an 800nm long m-NT assuming different  $\gamma$  values. The parameters used in the calculations are  $\kappa = 20\text{W/cmK}$ ,  $\tau = 22\text{fs}$  and  $\hbar\omega = 0.18\text{eV}$ . For the smallest  $\gamma$  values, the m-NT thermal coupling to the substrate is vanishingly small (less than 10% of the power generated along the tube is dissipated in the high bias through the substrate) and NDR is observed in the  $IV$  characteristics. As we increase  $\gamma$  to  $\sim 10^{11}\text{W/cm}^3\text{K}$  saturation is observed. If we further increase  $\gamma$ , the saturation is overcome but deviations from

the linear regime still arise. Our results clearly indicate that in the low bias regime, thermal effects can be neglected, but the high bias regime is basically governed by the m-NT capability for heat removal. Hence, the features of the electrical characteristics depend not only on the tube's length but also on  $\gamma$ . In Fig. 1(d) we plot the temperature difference  $\Delta T(0) = T(0) - T_0$  at the m-NT midlength as a function of the current for the set same of  $\gamma$ -values. Our model predicts that the larger the coupling coefficient  $\gamma$ , the higher current in the m-NT.

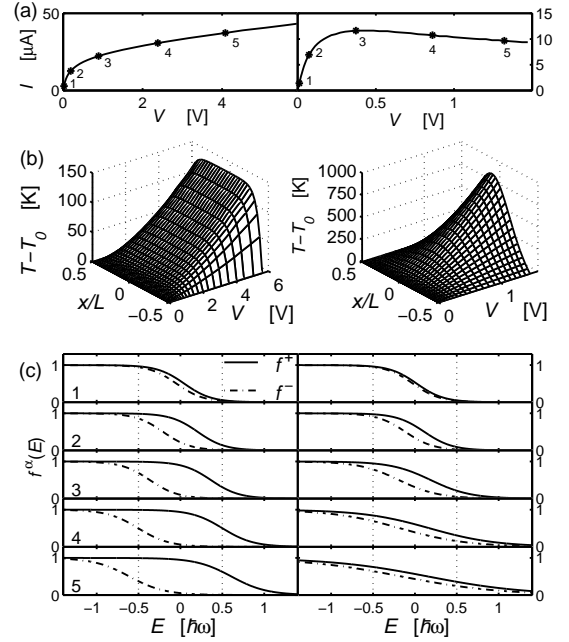


FIG. 2: Features comparison of 800nm long m-NT strongly (left) and weakly (right) coupled to the substrate: (a)  $IV$  characteristics; (b) Temperature profile  $\Delta T(x)$  as a function of the voltage  $V$ ; (c) Fermi distribution at midlength for each of the carrier branches at different points indicated in the  $IV$  characteristics. The distance between dashed line corresponds to the optical phonon energy.

In Fig. 2, we consider the situation of an 800nm long m-NT in two thermal coupling regimes i.e. i) strongly coupled (SST with  $\gamma = 10^{12}\text{W/cm}^3\text{K}$ , left hand side of Fig. 2) and ii) weakly coupled (FST with  $\gamma = 10^9\text{W/cm}^3\text{K}$ , right hand side of Fig. 2) to the substrate. In the SST, the  $IV$  characteristic exhibits a nonlinear behavior with high resistance at high fields (Fig. 2.a. LHS). In this case, the substrate acts as a heat sink, providing efficient dissipation of the heat produced along the tube while keeping both the electric field and power dissipated per unit volume low. This efficient heat removal reduces the temperature rise in the m-NT, thereby favoring relatively high current levels while maintaining a quasi uniform temperature profile along the tube (except at the edges) as shown in the LHS of Fig. 2.b. The LHS of Fig. 2.c displays the profile of the (Fermi-like)

carrier distributions at the NT mid-length for electrons with positive and negative Fermi velocity ( $f^+$  and  $f^-$ ) at the different points indicated along the  $IV$  curve in Fig. 2.a (LHS). No significant heating is observed before the separation between the two distribution quasi-Fermi levels becomes comparable to the optical phonon energy ( $E_F^+ - E_F^- \approx \hbar\omega$ ). Hence, the nonlinear behavior observed in this kind of configuration is basically attributed to the smooth onset of optical phonon scattering [8, 13], despite minor thermal broadening induced by Joule heating on the carrier distributions. In the FST, the  $IV$  characteristic exhibits a NDR at relatively low biases (Fig. 2.a RHS), and the current level is lower than in the previous case of strong thermal coupling. Because of poor heat removal, temperature rises rapidly with external biases manifesting a pronounced maximum at NT mid-length (RHS of Fig. 2.b). One notices the different scales on the voltage and temperature axis between the SST (LHS) and FST (RHS). Simultaneously, the Fermi distributions  $f^+$  and  $f^-$  remain weakly separated but experiencing significant heating even at low voltages as shown in Fig. 2.c (RHS) for the set of points along the  $IV$  characteristic on Fig. 2.a (RHS). The fast rise of temperature, consequence of the poor heat removal, locally broadens the electron distributions, and therefore enhances the scattering locally even at low bias. The rapid onset of non-uniform  $T$ -profile induces nonlinearities in the electric field, which result in a current diminution in order to satisfy the boundary conditions on the applied voltage at the NT contacts.

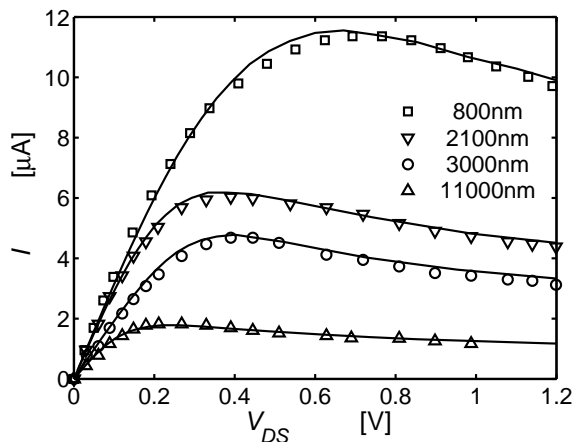


FIG. 3: Comparison between the  $IV$  characteristics for FSTs of different length calculated with our model (lines) and experimental data (symbols) of Ref. [11].

In Fig. 3 we compare the results of our model for FSTs with the experimental data of Ref. [11], for a which good agreement is observed for all NT-lengths. The physical parameters used in the calculations are  $\hbar\omega = 0.18\text{eV}$  and  $\kappa_{RT} = 20\text{W/cmK}$ . The relaxation time ( $\tau \sim 30\text{fs}$ ) used to compute the characteristics increases with diameter consistently with theoretical predictions [15], and lies

within previous experimental estimates [8, 9, 10]. Our model also assumes the presence of a contact resistance ( $R_c \sim 20\text{k}\Omega$ ).

In conclusion our model shows that the high field transport properties of m-NTs are strongly controlled by the onset of thermal effects, which can be altered by modifying the experimental setup. Using realistic parameters, our model is able to reproduce the  $IV$  characteristics in both substrate-supported and free-standing nanotubes. However the nonlinear behavior observed in each of the systems is caused by different phenomena affecting the carrier distribution. In the former, the transport features are due to an imbalance in the carrier population with positive and negative Fermi velocities associated with strong scattering and high current levels. In the latter, the NDR is attributed to strong scattering enhancement due to the broadening of the carrier distribution with low current level.

This work was supported by the Beckman Institute and Network for Computational Nanotechnology under NSF Grant # ECC-0228390.

\* Electronic address: jleburto@uiuc.edu

- [1] S. Iijima, Nature (London) **354**, 56 (1991).
- [2] R. Saito, G. Dresselhaus, and M. Dresselhaus, "Physical Properties of Carbon Nanotubes," Imperial College Press, London, (1998).
- [3] J. W. Mintmire, B. I. Dunlap, and C. T. White, Phys. Rev. Lett. **68**, 631 (1992).
- [4] Saito, M. Fujita, G. Dresselhaus, and M. S. Dresselhaus, Appl. Phys. Lett. **60**, 2204 (1992).
- [5] S. J. Tans, M. H. Devoret, H. Dai, A. Thess, R. E. Smalley, L. J. Geerligs, and C. Dekker, Nature (London) **386**, 474 (1997).
- [6] R. Martel, T. Schmidt, H. R. Shea, T. Hertel, and Ph. Avouris, Appl. Phys. Lett. **73**, 2447 (1998).
- [7] P. L. McEuen, M. S. Fuhrer, H. Park, IEEE Transactions on Nanotechnology, **1**, 78 (2002).
- [8] Z. Yao, C. L. Kane, and C. Dekker, Phys. Rev. Lett. **84**, 2941 (2000).
- [9] A. Javey, J. Guo, M. Paulsson, Q. Wang, D. Mann, M. Lundstrom, and H. Dai, Phys. Rev. Lett. **92**, 106804 (2004).
- [10] J.Y. Park, S. Rosenblatt, Y. Yaish, V. Sazonova, H. Üstünel, S. Braig, T.A. Arias, P.W. Brouwer, P.L. McEuen, Nano Lett. **4**, 517 (2004).
- [11] E. Pop, D. Mann, J. Cao, Q. Wang, K. Goodson, and H. Dai Phys. Rev. Lett. **95**, 155505 (2005).
- [12] L. C. Venema, J. W. Janssen, M. R. Buitelaar, J. W. G. Wildöer, S. G. Lemay, L. P. Kouwenhoven, and C. Dekker, Phys. Rev. B **62**, 5238 (2000).
- [13] M. A. Kuroda, A. Cangelaris, and J.-P. Leburton, Phys. Rev. Lett. **95**, 266803 (2005).
- [14] M. A. Osman and D. Srivastava, Nanotechnology **12**, 21 (2001).
- [15] M. Lazzeri, S. Piscanec, F. Mauri, A. C. Ferrari, and J. Robertson, Phys. Rev. Lett. **95**, 236802 (2005).